JOC The Journal of Organic Chemistry

Article

pubs.acs.org/joc

Experimental Measurement and Theory of Substituent Effects in π-Hydrogen Bonding: Complexes of Substituted Phenols with Benzene

Valia Nikolova,[†] Sonia Ilieva,[†] Boris Galabov,*,[†] and Henry F. Schaefer III*,[‡]

[†]Department of Chemistry, University of Sofia, 1 James Bourchier Avenue, Sofia 1164, Bulgaria

[‡]Center for Computational Quantum Chemistry, University of Georgia, Athens, Georgia 30602, United States

S *Supporting Information*

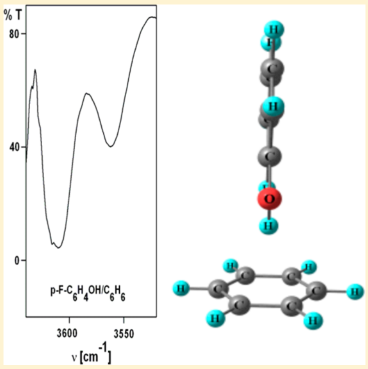

ABSTRACT: IR spectroscopic experiments and theoretical DFT computations reveal the effects of aromatic substituents on π-hydrogen bonding between monosubstituted phenol derivatives and benzene. Simultaneous formation of two π-hydrogen bonds (red-shifting O−H···π and blue-shifting *ortho*-C−H···π) contribute to the stability of these complexes. The interaction of the acidic phenol O−H proton-donating group with the benzene π-system dominates the complex formation. The experimental shifts of O−H stretching frequencies for the different phenol complexes vary in the range 45−74 cm^{-1}. *Strong* effects on hydrogen-bonding energies and frequency shifts of electron-withdrawing aromatic substituents and *very weak* influence of electron-donating groups have been established. Experimental quantities and theoretical parameters are employed in rationalizing the properties of these complexes. The acidities of the proton-donating phenols describe quantitatively the hydrogen-bonding process. The results obtained provide clear evidence that, when the structural variations are in the proton-donating species, the substituent effects on π-hydrogen bonding follow classic mechanisms, comprising both resonance and direct through-space influences. The performance of three alternative DFT functionals (B3LYP, B97-D, and PBE0 combined with the 6-311++G(2df,2p) basis set) in predicting the O−H frequency shifts upon complexation is examined. For comparison, O−H frequency shifts for several complexes were also determined at MP2/6-31++G(d,p).

■ INTRODUCTION

π-Hydrogen bonding is essential in understanding biochemical processes, such as protein folding, hydrophobic interactions, cluster and micelle formation, and protein−protein, protein−DNA, and ligand−bioreceptor interactions.[1−10] This type of complexing is also of key importance in supramolecular and host−guest chemistry and various areas of materials chemistry.[11−16] The introduction of substituents is the usual method for fine-tuning the strength and geometry of noncovalent interactions and is widely applied in the design of bioactive compounds and materials with special properties. The characterization of substituent effects in noncovalent interactions of aromatic systems has been the subject of alternative interpretations. More often, variations in the π-electron densities over the aromatic ring was considered as the underlying factor determining the strength of these interactions.[17−19]

However, recent theoretical studies of Wheeler and Houk[20−25] revealed that the perturbations of the π-electron cloud over the ring play only a minor role in these phenomena. Instead, a direct through-space interaction between the polar aromatic substituents with the approaching complexing agent (cation, anion, proton donor) determines the bonding energies of the formed complexes. The nature of the intermolecular forces involved in noncovalent interactions has also been the subject of alternative interpretations. Symmetry adapted perturbation theory (SAPT)[26] computations have shown that the balance between attractive (electrostatic, dispersion, induction) and repulsive (exchange) terms defines the energies and the effects of aryl substituents on different types of noncovalent interactions involving aromatic systems.[27,28] Kim et al.[29] analyzed the substituent effects on benzene sandwich dimers and established that the overall interaction energy correlates with its electrostatic component. However, for polysubstituted benzene dimers Ringer and Sherrill[30] found that dispersion interactions dominate over electrostatic effects. An interesting finding of Kim et al.[29] was that both electron-withdrawing and electron-donating substituents increase the interaction energy. Similarly, a complicated picture of subtle interplay between electronic terms contributing to interaction energy emerges from theoretical studies for different types of X−H/π hydrogen bonding[31,32] In contrast to conventional hydrogen bonds, where the electrostatic forces usually dominate the interaction,[3,4,11,12] high-level ab initio computations (at the CCSD(T)/CBS level) of Morita et al.[32] on C−H/π hydrogen bonding of methane with several arenes underlined the importance of dispersion contribution to the total interaction energy. CCSD(T)/CBS theoretical investigations by Fijii

Received: March 30, 2014
Published: July 8, 2014

dx.doi.org/10.1021/jo500732m | *J. Org. Chem.* 2014, 79, 6823−6831

et al.[33] of complexes of halogenated methane with benzene also confirmed a dominant contribution of the dispersion term in these interactions, although electrostatic effects also play a significant role.

In a recent vibrational Stark spectroscopy and DFT study Saggu, Levinson, and Boxer[34] estimated experimentally the electrostatic interaction energies of π-hydrogen-bonded complexes of phenol with benzene and several benzene-based solvents. Comparison with DFT (B3LYP/6-31+G(d,p)) total binding energies revealed that these interactions are dominated by electrostatics. Boxer and co-workers extended their studies[35] to complexes of N−H and S−H bonds with aromatic proton acceptors and confirmed that the experimentally evaluated electrostatic binding energies are in close correspondence with the total computed interaction energies. OH/π interactions between water and aromatic proton acceptors have been the subject of both experimental and theoretical studies.[36−39] Fayer et al.[40] applied two-dimensional infrared vibrational echo spectroscopy in investigating the complexation between phenol and benzene in CCl_4 solution. These authors established that the dissociation time constant for the weak complex formed is just 8 picoseconds. In subsequent research the π-hydrogen-bonded complexes between deuterated phenol and several other monosubstituted benzenes were also characterized by 2D vibrational echo spectroscopy and DFT computations using B3LYP/6-31+G(d,p).[41,42]

The effect of aromatic substituents on the structure of π-hydrogen-bonded complexes has also been of considerable interest.[43−47] Experimental rotational spectra showed[43] that the π-hydrogen-bonded complex of HCl with benzene is a symmetric top and HCl lies along the C_6 axis. Similarly, an experimental gas-phase structure determination of the complex of fluorobenzene with HCl revealed[44] C_s symmetry with the hydrogen of the HF slightly tilted toward the para carbon, possessing higher electron density. Theoretical studies[44−48] of π-hydrogen-bonded complexes of other substituted benzenes with simple proton donors demonstrated, however, random special orientations of the proton donor molecule in the complexes formed. No satisfactory explanation has been offered for these theoretical findings. Mishra et al.[49] conducted a detailed theoretical investigation on the effect of aromatic substituents on C−H/π interactions between acetylene acting as a proton donor and benzene derivatives containing various polar groups ($-NO_2$, −CN, −COOH, −Br, −Cl, −OH, and $-NH_2$). Their results showed that, in accord with chemical reasoning, electron-withdrawing substituents reduce the interaction energy, while electron-donating groups lead to stronger π-hydrogen bonding. SAPT analyses of the terms contributing to the overall interaction energies have provided intriguing results. The dispersive and electrostatic interactions were shown to be the principal driving forces in complex formation. However, the sum of dispersive, exchange, and inductive terms was in all cases near 0. Thus, the total energy of hydrogen bonding changed in line with the variations of the electrostatic term. This finding is in harmony with earlier results from Morokuma energy decomposition analysis[50] on conventional hydrogen bonding for complexes of carbonyl and nitrile derivatives with HF.[51]

In a recent theoretical study, Wheeler et al.[31] examined the effect of aromatic polar groups on prototypical X−H/π hydrogen bonding of BH_3, CH_4, NH_3, H_2O, and F−H proton donor species with substituted benzenes. Geometry constraints in the optimization processes were imposed to compare the impact of polar groups on interaction energies for the different systems considered. Nonetheless, the results of these authors provided useful qualitative insights into the nature of substituent effects in X−H/π interactions. SAPT energy decomposition computations revealed that electrostatic effects dominate N−H/π, O−H/π, and S−H/π interactions, while B−H/π and C−H/π interactions are strongly dependent on dispersion effects. The predicted impact of the substituent on N−H/π, O−H/π, and S−H/π hydrogen bonding was in harmony with physical expectations. Strong electron donating groups ($-NH_2$, $-OCHH_3$, $-N(CH_3)_2$) lead to distinctly higher interaction energies. Substituents possessing pronounced electron-withdrawing capacities (−CN, $-NO_2$, −CHO) lead to much weaker π-hydrogen bonding.

In early studies Yoshida et al.[52−54] investigated by IR spectroscopy series of complexes of phenol with the π-electrons of various unsaturated systems, including aromatic hydrocarbons and heteroaromatics. Seguin et al.[55] investigated by IR spectroscopy the association of substituted phenols with methylbenzenes. Their experimental approach was combined with CNDO/2 computations, which revealed a good correlation between the changes in aromatic π-electron densities and the shifts of O−H stretching frequencies. On the basis of these results, the authors proposed an electrostatic model in characterizing complex formation. Fujii et al.[56] applied IR spectroscopy and DFT computations (B3LYP/6-31G(d,p)) in examining the complexes of phenol with benzene, ethene, and ethyne. These authors established that the low-frequency shifts of the O−H band did not depend substantially on the type of π electrons. The theoretical computations for the phenol−benzene interaction showed that the structure of the complex is stabilized by the formation of O−H/π and *o*-C−H/π bonds directed at the midpoints of the aromatic CC bonds.

The theoretical studies in the literature on π-hydrogen bonding involving aromatic π-systems have mostly focused on analyzing the effect of substituents in the proton-accepting aromatic ring. It is therefore of substantial interest to examine and hopefully quantify the impact of substituents in the proton-donating species on these noncovalent interactions. In the present research, we applied FTIR spectroscopy and density functional theory (DFT) computations in investigating the effect of structural variations in the proton-donating moiety on π-hydrogen bonding. We focus on the interactions between monosubstituted phenols and benzene by considering an extended series of 20 proton-donating derivatives. The shifts of the phenolic O−H stretching frequency ($\Delta\nu_{OH}$) upon hydrogen bonding serve as an experimental measure of substituent effects. Unexpectedly, we found that, while electron-withdrawing groups exert quite a significant effect on $\Delta\nu_{OH}$, the influence of even strong electron-donating substituents is almost negligible. DFT computations and correlations with experimental quantities provided keys to understanding the origin of these unusual spectroscopic properties of π-hydrogen-bonded complexes.

■ METHODS

Computational Methods. DFT computations employing the B3LYP,[57] B97-D,[58] and PBE0[59] functionals combined with the 6-311++G(2df,2p) basis set[60] were applied in evaluating the structure, energetics, and properties of monomeric species and π-hydrogen-bonded complexes between proton-donating phenol derivatives and benzene. The B3LYP and PBE0 hybrid functionals and the B97-D GGA-type density functional with long-range dispersion corrections in combination with the basis set employed have been shown to describe satisfactorily hydrogen-bonding phenomena.[61] Harmonic vibrational frequency computations showed that all optimized structures are true minima on the pertinent potential energy surfaces. C_s symmetry is possible for many of the formed complexes. The symmetric

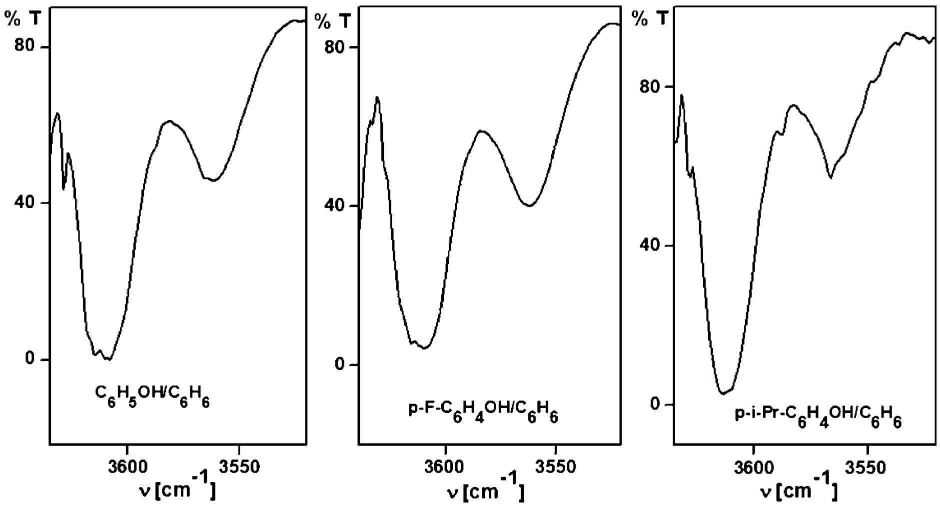

Figure 1. Monomeric and π-hydrogen-bonded phenolic O−H stretching bands in CCl_4 solution, containing 0.5 mol/L benzene. The concentrations of the phenols are below 0.01 mol/L.

optimizations led, however, to the presence of a very small (below 20 cm^{-1}) single imaginary frequency, except in a few cases. For consistency of approach, we consider hereafter the results from optimizations without imposed symmetry constraints. The interaction energies were corrected for basis set superposition errors by applying the counterpoise method of Boys and Bernardi.[62] To model the conditions of the IR spectroscopic experiments conducted, the properties of monomers and complexes were theoretically evaluated for simulated carbon tetrachloride solutions by applying the IEFPCM method.[63] Frequency shifts of the O−H stretching band for several complexes containing electron-donating and electron-withdrawing substituents were also evaluated at the MP2/6-31++G(d,p) level. All computations employed the Gaussian09 program package.[64]

NBO[65] and Hirshfeld[66] population analyses were applied in characterizing the effects of aromatic substituents. In addition, the electrostatic potentials at nuclei (EPN) were also determined. Politzer and Truhlar[67] defined the electrostatic potential at nucleus Y (V_Y) by the relation (in atomic units)

$$V_Y \equiv V(\mathbf{R}_Y) = \sum_{A(\neq Y)} \frac{Z_A}{|\mathbf{R}_A - \mathbf{R}_Y|} - \int \frac{\rho(\mathbf{r})}{|\mathbf{r} - \mathbf{R}_Y|} \, d\mathbf{r} \qquad (1)$$

In this expression, Z_A is the charge at nucleus A at position defined by the radius vector $\mathbf{R}_A$, and $\rho(\mathbf{r})$ is the electron density function. The singular term for nucleus Y is excluded. The EPN values were found to reliably describe the reactivity trends determined by structural variations. EPN was first proposed as a reactivity index in characterizing hydrogen-bonding properties of carbonyl and nitrile molecules.[68] This index was later applied in characterizing chemical reactivity and other properties of molecules.[69−71] In contrast to atomic charges, the electrostatic potential at nuclei is a rigorously defined quantum mechanical quantity. As already discussed, hydrogen bonding depends strongly on the electrostatic forces acting between the interacting molecules.[4,11,12] By definition, the V_Y values describe these forces at specific atomic sites of the monomer species considered. Although the EPN depends on the positive and negative charges of the entire molecule, the $1/\mathbf{r}$ dependence of V_Y (eq 1) exercises a much greater influence of the charges in close vicinity of the respective nucleus. These effects were recently analyzed in detail for a series of substituted benzenes.[72]

Experiments. FTIR spectra of the studied complexes in the 4000−3000 cm^{-1} region were recorded at 1 cm^{-1} resolution. Very dilute solutions (<0.01 M) of the phenol derivatives in CCl_4 were investigated to avoid intermolecular association. The concentration of benzene in all experiments was 0.5 M. A quartz cell of 1 cm path length was used. The phenols studied were commercial samples with purity above 98%, except for two derivatives: *p*-cyanophenol (>95%) and *m*-methoxyphenol (>96%). The phenols were dissolved in a ready 0.5 M solution of benzene in carbon tetrachloride. Because of the very low solubility of several phenols, saturated solutions at room temperature were investigated in these cases. The recorded spectra contain two bands in the O−H stretching region: a more intense band of a monomeric phenol derivative and a second O−H band, shifted to lower frequencies as result of complex formation. Figure 1 shows typical obtained IR spectra. No associative bands in the 3500−3200 cm^{-1} interval were observed. For a considerable number of phenols containing polar substituents, the intensities of the monomeric O−H stretching vibrational band and, especially, the O−H band in the π-hydrogen-bonded complexes were very low (see the IR spectra in the Supporting Information, Table S2).

■ RESULTS AND DISCUSSION

Structures of the Complexes. In contrast to substitution at the proton-accepting aromatic ring, which results in divergent special orientations of the proton-donating species in π-hydrogen bonding,[39−44] our computations revealed that the structures of all studied complexes between substituted phenols and benzene are very similar. The complexes possess a typical T-shaped structure with an almost perpendicular orientation of the proton donor with respect to the benzene plane (Figure 2). The simultaneous formation of two hydrogen bonds with the benzene π-system favors such a structure. The first hydrogen bond involves the phenol O−H bond and the second the ortho-positioned C−H bond. Figure 1 illustrates two well-separated O−H stretching bands for the cases of complexes of phenol, *p*-fluorophenol, and *p*-isopropylphenol with benzene. Intermolecular hydrogen bonds involving the OH group are typically characterized by wide O−H stretching bands, corresponding to the varying dissociation energies and divergent structures of the complexes.[3,11,12] As will be discussed later, the regularities in frequency shifts upon hydrogen bonding are also clear indications for the structural similarity of the complexes formed.

The theoretical computations also revealed that an alternative structure of the complexes could also be optimized with the O−H and C−H bonds pointing at the ring edges (Figure 3). The energy differences between these alternative structures are very small, less than 0.01 kcal/mol. Essentially, these different configurations exist simultaneously in CCl_4 solution with facile transitions between them. Two of these

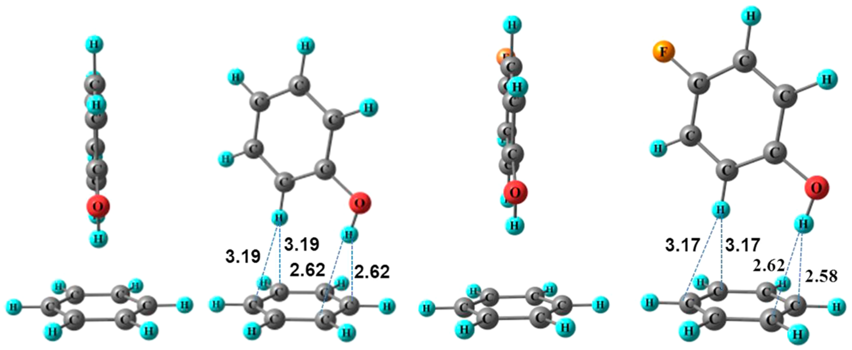

Figure 2. Optimized structures of *π*-hydrogen-bonded complexes of phenol (left) and *p*-fluorophenol (right) with C_6H_6.

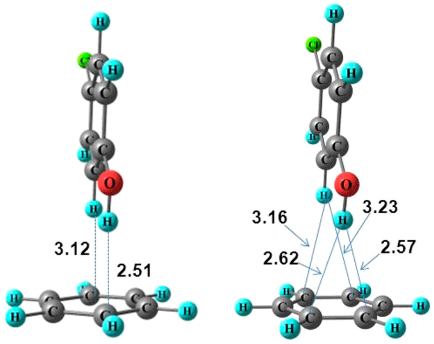

Figure 3. Alternative configurations of the *π*-hydrogen-bonded complex of *p*-chlorophenol with benzene from B3LYP/6-311++G(2df,2p) computations.

alternative structures of complexes (for *p*-NH_2 and *p*-*t*-octyl phenol derivatives) could not be optimized. The further interpretation in the present work employs results for the complexes with O−H and C−H bonds pointing to the middle of the aromatic CC bonds. In most cases, these structures have slightly lower energies. Conducted B97D/6-311++G(2df,2p) and PBE0/6-311++G(2df,2p) computations for the parent complex of phenol and benzene confirmed the two alternative complex structures (the optimized geometries are given in Tables S7, S9, and S10 in the Supporting Information).

The stronger O−H···*π* bonds are distinctly shorter (2.45 Å to the midpoint of the closest ring CC bond in the case of the phenol−benzene complex) than the weaker C−H···*π* bond (3.05 Å to the midpoint of the CC bond on the opposite side of the ring). Szatylovicz and Krygowski[73] investigated by DFT computations conventional hydrogen bonding of para-substituted phenols and phenolates with a model proton acceptor (fluoride ion) and donor (HF). They established very good correlations between binding energies and a bond strength parameter (BSP), defined in terms of distances between interacting atoms in the complexes.

The sharpness of the O−H IR band along the series of phenol−benzene complexes studied provides possibilities for accurate measurement of the substituent effects on the *π*-hydrogen bonding.

Red-Shifting and Blue-Shifting *π*-Hydrogen Bonds between Benzene and Substituted Phenols. Unusual trends for the shifts of O−H and C−H streching frequencies upon complexation were obtained. For the O−H stretchings both computations and experiment reveal considerable frequency lowering as result of the expected weakening of the O−H bond upon hydrogen bonding. The experimental frequency shifts vary from −44 to −74 cm^{-1} along the series (Table 1), depending on the nature of the phenol subsituent. The same O−H frequency shifts from B3LYP/6-311++(2df,2p) computations range from 59 to 95 cm^{-1}. A reverse trend for the C−H shifts was obtained from the theoretical evaluation of isolated C−H frequencies. These C−H shifts were determined from computations on molecules in which all ring hydrogens were replaced by deuterium except the *o*-C−H hydrogen involved in the hydrogen bonding. The estimated increase of C−H frequencies ranged from 2 to 12 cm^{-1} (Table 1). These computed $\Delta\nu_{CH}$ shifts reflect the much weaker *π*-hydrogen bonding with participation of C−H bonds.

The evaluated changes of bond lengths for the proton-donating bonds upon conplexation are given in Table S1 of the Supporitng Information. In harmony with the measured and computed O−H frequency shifts, the Δr_{OH} values reveal a distinct lengthening of the O−H bonds as result of complex formation. In contrast, the blue-shifting hydrogen bonding is associated with shortening and strengthening the C−H bonds. As already discussed, the usual red-shifting hydrogen bonding is dominated by electrostatic interactions between the monomers.[3,4,11,12] A contribution from charge transfer is also an important factor.[70] The process is accompanied by certain transfer of electron density from the proton acceptor to the antibonding *σ** X−H orbital of the proton donor, resulting in a weakened, elongated X−H bond and a spectroscopic red shift.[71] The blue-shifting hydrogen bonds, on the other hand, are dominated by the dispersive energy terms.[30−33,71] Hobza and Havlas[74] emphasized that the interaction between the monomers in this type of bonding is increased by contraction of the X−H bond, a secondary result of some charge transfer from the proton-accepting species to a remote part of the proton-donating species. Structural reorganization, following this charge transfer, leads to shortening and strengthening of the X−H bond and a blue shift of its stretching frequency. The theoretically evaluated total transfers of negative charge from the proton-accepting benzene to the proton-donating molecules are presented in the last column of Table 1. The charge transfer from the proton-accepting to the proton-donating species varies in harmony with the ν_{OH} changes. The correlation coefficient for the plot $\Delta\nu_{OH}^{theor}/\Delta q$ is 0.964. Strong electron-donating groups, such as $-NH_2$, cause a lesser degree of negative charge transfer (Δq for the *p*-aminophenol proton donor is 0.0035 e). Strong electron-withdrawing groups, such as $-NO_2$ and −CN, attract much greater electron dnesity (Δq for *p*-nitrophenol is 0.0084 and 0.0074 e in the case of *p*-cyanophenol).

Substituent Effects in *π*-Hydrogen Bonding. Numerous investigations[24,25,31−47] have revealed that polar groups

Table 1. Complexes between Substituted Phenol and Benzene: Experimental and Computed O−H and Isolated *o*-C−H IR Stretching Frequency Shifts (cm^{-1}) and Negative Charge Transfer (in e) from Proton-Accepting to Proton-Donating Species for π-Hydrogen-Bonded Structures[a]

substituent	ν_{OH}^{exptl} monomer	$\nu_{OH}^{exptl\,b}$ complex	$\Delta\nu_{O-H}^{exptl\,b}$	$\Delta\nu_{OH}^{theor}$	ν_{C-H}^{theor} monomer	ν_{CH}^{theor} complex	$\Delta\nu_{C-H}^{theor}$	Δq NBO
H (phenol)	3610	3562	−48	−65	3157	3168	+11	0.0047
p-$CH(CH_3)_2$	3611	3566	−45	−65	3161	3166	+5	0.0044
p-CH_3	3611	3566	−45	−65	3157	3164	+7	0.0044
p-$OCHH_3$	3615	3568	−47	−60	3165	3169	+4	0.0017
p-$C(CH_3)_3$	3610	3565	−45	−63	3155	3162	+7	0.0043
p-*n*-octyl	3610	3566	−44	−59	3154	3163	+10	0.0042
p-*t*-octyl	3610	3565	−45	−61	3157	3164	+7	0.0043
p-NH_2	3612	3567	−45	−61	3158	3165	+6	0.0035
p-$NHCOCH_3$	3612	3567	−45	−66	3165	3169	+3	0.0050
p-F	3611	3563	−48	−73	3168	3175	+7	0.0054
m-$OCHH_3$	3609	3563	−46	−63	3165	3176	+12	0.0034
p-Cl	3608	3555	−53	−72	3167	3176	+8	0.0059
p-Br	3607	3554	−53	−76	3167	3173	+6	0.0061
p-F	3606	3554	−52	−75	3173	3177	+5	0.0052
m-Cl	3605	3550	−55	−76	3170	3175	+4	0.0059
p-CHO	3606	3539	−67	−89	3177	3174	+2	0.0069
p-$COCH_3$	3605	3543	−62	−81	3168	3174	+6	0.0062
p-CF_3	3603	3546	−57	−81	3170	3177	+7	0.0066
p-CN	3604	3537	−67	−86	3172	3177	+6	0.0074
p-NO_2	3604	3530	−74	−97	3175	3180	+5	0.0081

[a] All computed values refer to simulated solutions in CCl_4, with the B3LYP/6-311+G(2dp,2p) basis set. [b] In CCl_4 solution.

attached to the *proton-accepting aromatic rings* induce considerable changes in π-hydrogen-bonding energies. Further, it has been demonstrated that direct through-space interactions of the substituents with the incoming proton-donor species dominate these processes.[24,25,31] Our experiments show that the impact of electron-releasing groups on the spectroscopic properties of complexes involving *aromatic substitution in the proton-donating species* is surprisingly small, almost negligble. We define the experimental frequency shifts of the O−H stretching band ($\Delta\nu_{OH}^{exptl}$) upon hydrogen bonding as a quantitative measure of substituent effects. Table 1 presents the experimental O−H frequencies for monomeric phenols and for hydrogen-bonded complexes of these phenols with benzene in CCl_4 solution. It is seen that the frequency shifts ($\Delta\nu_{OH}^{exptl}$) invoked by electron-donating groups such as CH_3, $CH(CH_3)_2$, OCH_3, and NH_2 are very small. The frequency shifts upon complexation induced by these substituents differ from the case of unsubstituted phenol by only 1−3 cm^{-1}. On the other hand, strong electron-withdrawing groups cause very significant increases in $\Delta\nu_{OH}^{exp}$. The frequency shifts in the presence of the *p*-CN, *p*-CHO, and *p*-NO_2 groups are quite high at 67−74 cm^{-1} in comparison with the analogous value for phenol (48 cm^{-1}) (Table 1). These trends are observed throughout the complexes studied. Understanding the physical nature of these substituent effects was, therefore, of principal interest in our research.

Correlation with the Hammett constants[75] is the usual approach in resolving the mechanisms of influence of aromatic substituent groups in various molecular interactions. Theoretical computations can also provide important tools in characterizing the effects of substituents. Table 2 presents the computed interaction energies (at the B3LYP/6-311G(2df,2p) level) for the complexes considered. Experimental constants characterizing the substituted phenols, as well as theoretical parameters (Table 2), are expected to provide insights into the impact of polar groups in these intermolecular processes. All theoretical quantities were determined for simulated CCl_4 solution, in accordance with our spectroscopic experiments. Table 2 contains also the experimentally measured substituent effects as expressed by the $\Delta\nu_{OH}^{exptl}$ values. The correlations of $\Delta\nu_{OH}^{exptl}$ with the standard Hammett σ constants did not produce satisfactory results (correlation coefficient r = 0.822, Table 2). This problem certainly arises from the very weak effects of electron-donating groups as opposed to the quite significant impact of electron-withdrawing substituents. These unexpected observations contradict, at first sight, chemical intuition and need special attention. The phenol proton-donating species considered contain an electronegative center, the OH oxygen, which is able to engage in *enhanced resonance* with strong electron-withdrawing groups at the para position in the aromatic ring. Such interactions are well represented by the set of σ^- constants.[75] The relationship between the σ^- constants and $\Delta\nu_{OH}^{exptl}$ is characterized by a much improved correlation coefficient (r = 0.963). Thus, the specific intrinsic interactions in the proton-donating phenols appear to control the π-hydrogen bonding with the proton-accepting benzene molecule.

A definitive explanation of the substituent effects on frequency shifts comes by exploring the relationship between $\Delta\nu_{O-H}^{exptl}$ and the experimental pK_a values for the phenols considered.[76] An excellent correlation between these two quantities was obtained, with the correlation coefficient r = 0.991 (Table 2). The plot between $\Delta\nu_{O-H}^{exptl}$ and pK_a is illustrated in Figure 4. This result shows that the acidities of the proton-donating molecules are a key element in the substituent impact on OH/π bonding. More acidic phenols form stronger complexes, resulting in greater O−H frequency shifts. Thus, classic chemical reasoning and intuition may successfully explain the behavior of the proton donor and acceptor species. As already discussed, theoretical studies[20−25] earlier demonstrated that through-space effects of substituents dominate these interactions for complexes with structural variations in the

Table 2. BSSE Corrected Interaction Energies (kcal/mol) for π-Hydrogen-Bonded Complexes of Substituted Phenols and Benzene (B3LYP/6-311++G(2df,2p)), Experimental IR Frequency Shifts (cm^{-1}), Computed IR Intensities (A_{O-H}, km/mol), σ and σ^- Substituent Constants, Experimental pK_a Values, Theoretically Estimated NBO and Hirshfeld Atomic Charges (in e), and Shifts of Electrostatic Potential at Nuclei (ΔV_H, kcal/mol)[a]

substituent	ΔE_{cor}^{theor}	$\Delta\nu_{O-H}^{exptl}$	A_{O-H}^{theor}	σ^b	$\sigma^{-\,b}$	p$K_a^{exptl\,c}$	q_H NBO	q_H Hirsh	ΔV_H^d
H (phenol)	−0.732	−48	376	0	0	9.99	0.4795	0.1748	0.00
p-CH(CH$_3$)$_2$	−0.786	−45	381	−0.15	−0.15	10.3	0.4787	0.1734	−2.56
p-CH$_3$	−0.845	−45	371	−0.17	−0.17	10.19	0.4786	0.1733	−2.62
p-OCHH$_3$	−0.653	−47	375	−0.27	−0.26	10.21	0.4780	0.1721	−3.93
p-C(CH$_3$)$_3$	−0.751	−45	379	−0.13	−0.13	10.30	0.4787	0.1734	−2.77
p-*n*-octyl	−0.735	−44	367	-	-	10.38	0.4785	0.1730	−3.48
p-*t*-octyl	−0.754	−45	387	-	-	10.33	0.4784	0.1731	−2.87
p-NH$_2$	−0.748	−45	350	−0.66	−0.15	10.3	0.4769	0.1702	−7.16
p-NHCOCH$_3$	−0.950	−45	406	0.21	0.21	10.1	0.4801	0.1752	−0.24
p-F	−0.990	−48	392	0.06	−0.03	9.95	0.4804	0.1763	4.23
m-OCHH$_3$	−0.697	−46	391	0.12	0.12	9.93	0.4780	0.1721	−3.93
p-Cl	−0.970	−53	424	0.23	0.19	9.38	0.4815	0.1782	6.93
p-Br	−1.093	−53	445	0.23	0.25	9.34	0.4817	0.1785	7.50
m-F	−1.152	−52	420	0.34	0.34	9.28	0.4824	0.1790	6.72
m-Cl	−1.061	−55	451	0.37	0.37	9.02	0.4823	0.1793	7.63
p-CHO	−1.274	−67	544	0.42	1.03	7.66	0.4844	0.1835	15.64
p-COCH$_3$	−1.121	−62	501	0.5	0.84	8.05	0.4830	0.1813	11.68
p-CF$_3$	−1.206	−57	466	0.54	0.65	8.68	0.4835	0.1817	12.85
p-CN	−1.289	−67	543	0.66	1	7.95	0.4853	0.1845	18.66
p-NO$_2$	−1.459	−74	611	0.78	1.27	7.15	0.4868	0.1871	22.50
r, corr coeff with ΔE^{cor}		0.904	0.916	0.867	0.941	0.918	**0.972**	**0.967**	**0.963**
r, corr coeff with $\Delta\nu_{O-H}^{exptl}$			**0.984**	0.822	**0.963**	**0.991**	**0.945**	**0.954**	**0.961**

[a] All computed quantities refer to simulated CCl_4 solution. [b] From ref 75. [c] From ref 76. [d] $\Delta V_H = V_H(R) - V_H(\text{phenol})$.

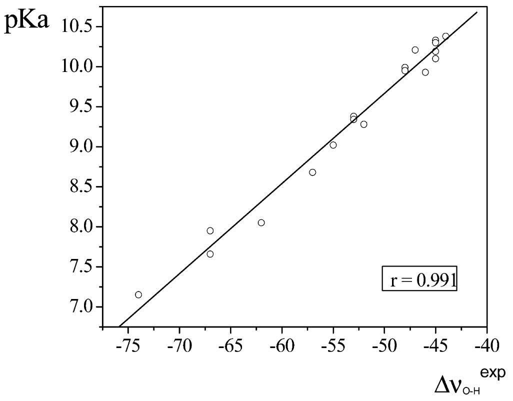

Figure 4. Relationship between experimental frequency shifts $\Delta\nu_{O-H}^{exptl}$ (cm^{-1}) and pK_a values for hydrogen-bonded complexes of substituted phenols and benzene.

proton-accepting aromatic ring, while the classic resonance effects have only a minor influence. It is interesting that the theoretically estimated IR intensities for the O−H stretching band (A_{OH}) in the complexes correlate very well ($r = 0.984$) with the measured O−H frequency shifts (Table 2). It appears that this usually neglected property may well serve in analyzing substituent effects in hydrogen bonding. As expected, the intensities of the O−H band are much enhanced upon complex formation (see Table S1 in the Supporting Information).

Further insights into the nature of substituent influence for the systems examined in the present work comes from the derived relationships between π-hydrogen bonding energies and theoretical parameters, characterizing the properties of the O−H proton donor center. NBO and Hirshfeld atomic charges for the O−H hydrogen (q_H) were evaluated at the level of theory employed. In addition, the electrostatic potential potentials at the same atom (V_H) were also determined. These molecular parameters and the BSSE and zero-point vibrational energy corrected interaction energies (ΔE_{cor}) are presented in Table 2. The linear regression correlation coefficients for the plots of ΔE_{cor} with q_H and V_H are given in the last row of the table. We underline here that because of the complex character of interaction between the phenols and benzene with simultaneous formation of two π-hydrogen bonds, no perfect correlation between ΔE_{cor} and the theoretical parameters considered (describing O−H properties only) can be expected. The simultaneous formation of OH/π and CH/π bonds encompasses different types of energy contributions, which may not necessarily vary in a synchronous way. Nonetheless, quite satisfactory correlations between ΔE_{cor} and q_H(NBO) ($r = 0.970$) and q_H(Hirshfeld) ($r = 0.965$) atomic charges were derived. Similarly, the variation of ΔE_{cor} is well predicted by the shifts of the EPN values ($r = 0.961$) for the O−H hydrogen, represented as the change of V_H between the substituted derivative and unsubstituted phenol ($\Delta V_H = V_H(R) - V_H(\text{phenol})$). These relationships display the dominant contribution of OH/π bonding and also the significance of electrostatic interactions on the overall binding energy.

Generalizing, the examination of substituent impact on π-hydrogen bonding for a series of phenols with benzene reveals that classic intrinsic interactions in the proton-donating molecules, such as resonance and field/inductive effects, dominate these processes. The experimentally measured substituent effects, as expressed by the O−H stretching frequency shifts upon complexation, correlate quantitatively with phenol acidities. Correlations with Hammett constants confirm the role of enhanced resonance in the proton-donating species as an important factor in determining these noncovalent interactions.

Frequency Shifts from Alternative DFT Functionals. Thus, far we have based our discussion on theoretical data from B3LYP/6-311++G(2df,2p) computations. It was of interest to test alternative DFT functionals, especially their ability to predict the O−H frequency shifts, induced by π-hydrogen bonding. Two further DFT functionals—B97-D[58] and PBE0[59]—were applied in evaluating the frequencies for isolated monomer phenols and their complexes with benzene. Both of these functionals have been applied in characterizing noncovalent interactions and found to describe satisfactorily hydrogen bonding.[61] The basis set described above was employed. Table 3 compares the performance of the tested functionals in evaluating $\Delta\nu_{OH}$. No scaling of frequencies was applied. Overall, these density functionals provide similarly good correlations with the experimentally measured low-frequency shifts for the O−H stretching vibration. The correlation coefficients for the plot of $\Delta\nu_{OH}^{theor}$ vs $\Delta\nu_{OH}^{exptl}$ are 0.963 for B3LYP, 0.968 for B97-D, and 0.967 for PBE0 computations. The best correlation between $\Delta\nu_{OH}^{theor}$ abd $\Delta\nu_{OH}^{exptl}$ is obtained using the B97-D functional. Somewhat surprisingly, the B3LYP functional performed better than the other two methods with respect to the estimated magnitude of frequency shifts.

Table 3. Theoretical vs Experimental O−H Frequency Shifts (cm^{-1}) upon π-Hydrogen Bonding between Substituted Phenols and Benzene from DFT Computations Employing the B3LYP, B97D, and PBE0 Functionals and the 6-311++G(2df,2p) Basis Set

	$\Delta\nu_{O-H}$			
substituent	MP2	B97-D	PBE0	exptl
H (phenol)	−65	−85	−95	−48
p-CH(CH$_3$)$_2$	−65	−85	−94	−45
p-CH$_3$	−65	−86	−93	−45
p-OCHH$_3$	−60	−80	−89	−47
p-C(CH$_3$)$_3$	−63	−81	−92	−45
p-*n*-octyl	−59	−82	−89	−44
p-*t*-octyl	−64	−83	−93	−45
p-NH$_2$	−61	−80	−88	−45
p-NHCOCH$_3$	−66	−92	−97	−45
p-F	−73	−92	−102	−48
m-OCHH$_3$	−63	−82	−97	−46
p-Cl	−72	−96	−105	−53
p-Br	−76	−97	−108	−53
m-F	−75	−99	−107	−52
m-Cl	−76	−99	−109	−55
p-CHO	−89	−121	−124	−67
p-COCH$_3$	−81	−104	−116	−62
p-CF$_3$	−81	−103	−115	−57
p-CN	−86	−116	−122	−67
p-NO$_2$	−97	−128	−131	−74
r, corr with $\Delta\nu_{OH}^{exptl}$ [a]	**0.963**	**0.968**	**0.967**	

[a] Correlation coeffcients for the relationships between theoretical and experimental frequency shifts for the O−H stretching vibration.

Table 4. Theoretical vs Experimental O−H Frequency Shifts (cm^{-1}) upon π-Hydrogen Bonding for Selected Phenols and Benzene from MP2/6-31++G(d,p) Computations

	$\Delta\nu_{O-H}$	
substituent	MP2	exptl
H (phenol)	−73	−48
p-CH$_3$	−71	−45
p-NH$_2$	−73	−45
p-Cl	−79	−53
p-CN	−90	−67

We also conducted MP2/6-31++G(d,p) computations for several complexes of the studied series. The obtained frequency shifts upon complexation are presented in Table 4. In general, the trends established are in harmony with the results from application of density functional theory methods.

■ SUMMARY AND CONCLUSIONS

IR spectroscopy and density functional theory reveal the nature of substituent effects in π-hydrogen bonding for the interactions of substituted phenols as proton donors and benzene as proton acceptors. O−H/π and *o*-C−H/π hydrogen bonds are simultaneously formed, increasing the dissociation energy of the complexes. The *strong* effect of electron-withdrawing groups and *very weak* influence of electron-donating substituents characterize the interactions, as reflected in the O−H low-frequency shifts ($\Delta\nu_{OH}$) and binding energies. These unusual features, established from both experiment and theory, find plausible explanation in the established excellent correlation (correlation coefficient $r = 0.991$) for the plot between experimental $\Delta\nu_{OH}$ and the phenol pK_a values. The computed interaction energies correlate satisfactorily with NBO and Hirshfeld atomic charges for the O−H hydrogen as well as with electrostatic potential at nuclei values (V_H). Among three tested DFT functionals, B3LYP, B97-D, and PBE0, combined with the 6-311++G(2df,2p) basis set, the B97-D computations provide the best correlation with the experimental $\Delta\nu_{OH}^{exptl}$ values for CCl_4 solutions of the complexes. The B3LYP predictions, however, are closest to experiment with respect to the magnitude of O−H frequency shifts.

In contrast to some literature conclusions concerning the substituent impact on π-hydrogen bonding for systems with structural variations in the proton-accepting benzene rings, the present results demonstrate that both resonance and through-space effects characterize the influence of polar groups in these noncovalent interactions, involving different substitution at the proton-donating species.

■ ASSOCIATED CONTENT

Supporting Information

Table S1, containing calculated geometry parameters and IR intensities of the O−H stretching band, Table S2, containing FTIR spectra of all studied complexes in CCl_4, Tables S3−S9, giving energies and Cartesian coordinates of all optimized geometric structures, and text giving the complete ref 64. This material is available free of charge via the Internet at http://pubs.acs.org.

■ AUTHOR INFORMATION

Corresponding Author

*E-mail for B.G.: galabov@chem.uni-sofia.bg.
*E-mail for H.F.S.: qc@uga.edu.

Notes

The authors declare no competing financial interest.

■ ACKNOWLEDGMENTS

B.G. thanks the Center for Computational Quantum Chemistry, University of Georgia, for supporting his stay during 2013. The research in Georgia was supported by the U.S. National Science Foundation, grant CHE-1361178. The research in Sofia was supported by EU grant FP7-REGPOT-2011-1 (project BeyondEverest).

■ REFERENCES

(1) Levitt, M.; Perutz, M. F. *J. Mol. Biol.* **1988**, *201*, 751−754.

(2) Sheinerman, F. B.; Honig, B. *J. Mol. Biol.* **2002**, *318*, 161−177.

(3) Desiraju, G. R.; Steiner, T. *The Weak Hydrogen Bond in Structural Chemistry and Biology*; Oxford University Press: New York, 2001.

(4) Naray-Szabo, G. In *Molecular Electrostatic Potentials: Concepts and Applications*; Murray, J. S., Sen, K., Eds.; Elsevier: Berlin, 1996; pp 333−365.

(5) Apaya, R. P.; Lucchese, B.; Price, S. L.; Vinter, J. G. *J. Comput. Aided Mol. Des.* **1995**, *9*, 33−43.

(6) Gilson, M. K.; Zhou, H. X. *Annu. Rev. Biophys. Biomol. Struct.* **2007**, *36*, 21−42.

(7) Leach, A. R.; Shoichet, B. K.; Peishoff, C. E. *J. Med. Chem.* **2006**, *49*, 5851−5855.

(8) Faver, J. C.; Benson, M. L.; He, X.; Roberts, B. P.; Wang, B.; Marshall, M. S.; Kennedy, M. R.; Sherrill, C. D.; Merz, K. M. *J. Chem. Theory Comput.* **2011**, *7*, 790−797.

(9) Zheng, H.; Comeforo, K.; Gao, J. *J. Am. Chem. Soc.* **2009**, *131*, 18−19.

(10) Ozawa, T.; Okazaki, K.; Kitaura, K. *Org. Biomol. Chem.* **2011**, *19*, 5231−5237.

(11) Jeffrey, G. A. *An Introduction to Hydrogen Bonding*; Oxford University Press: New York, 1997.

(12) Grabowski, S. J. *Hydrogen Bonding: New Insights*; Springer: New York, 2006.

(13) Schneider, H.-J.; Yatsimirski, A. K. *Principles and Methods in Supramolecular Chemistry*; Wiley: Chichester, U.K., 2000.

(14) Hunter, C. A.; Lawson, K. R.; Perkins, J.; Urch, C. J. *J. Chem. Soc., Perkin Trans. 2* **2001**, 651−669.

(15) Knowles, R. R.; Jacobsen, E. N. *Proc. Natl. Acad. Sci. U.S.A.* **2010**, *107*, 20678−20685.

(16) Verma, M.; Chaudhry, A.; Fahrni, C. J. *Org. Biomol. Chem.* **2009**, *7*, 1536−1546.

(17) Hunter, C. A.; Sanders, J. K. M. *J. Am. Chem. Soc.* **1990**, *112*, 5525−5534.

(18) Hunter, C. A.; Lawson, K. R.; Perkins, J.; Urch, C. J. *J. Chem. Soc., Perkin Trans. 2* **2001**, 651−669.

(19) Cockroft, S. L.; Perkins, J.; Zonta, C.; Adams, H.; Spey, S. E.; Low, C. M. R.; Vinter, J. G.; Lawson, K. R.; Urch, C. J.; Hunter, C. A. *Org. Biomol. Chem.* **2007**, *5*, 1062−1080.

(20) Wheeler, S. E.; Houk, K. N. *J. Am. Chem. Soc.* **2008**, *130*, 10854−10855.

(21) Wheeler, S. E.; McNeil, A. J.; Müller, P.; Swager, T. M.; Houk, K. N. *J. Am. Chem. Soc.* **2010**, *132*, 3304−3311.

(22) Wheeler, S. E.; Houk, K. N. *J. Phys. Chem. A* **2010**, *114*, 8658−8664.

(23) Wheeler, S. E. *J. Am. Chem. Soc.* **2011**, *133*, 10262−10274.

(24) Raju, R. K.; Bloom, J. W. G.; An, Y.; Wheeler, S. E. *ChemPhysChem* **2011**, *12*, 3116−3130.

(25) Wheeler, S. E. *Acc. Chem. Res.* **2013**, *46*, 1029−1038.

(26) Jeziorski, B.; Moszynski, R.; Szalewicz, K. *Chem. Rev.* **1994**, *94*, 1887−1930.

(27) Sinnokrot, M. O.; Sherrill, C. D. *J. Phys. Chem. A* **2003**, *107*, 8377−8379.

(28) Sinnokrot, M. O.; Sherrill, C. D. *J. Am. Chem. Soc.* **2004**, *126*, 7690−7697.

(29) Lee, E. C.; Kim, D.; Jurecka, P.; Tarakeshwar, P.; Hobza, P.; Kim, K. S. *J. Phys. Chem. A* **2007**, *111*, 3446−3457.

(30) Ringer, A. L.; Sherrill, C. D. *J. Am. Chem. Soc.* **2009**, *131*, 4574−4575.

(31) Bloom, J. W. G.; Raju, R. K.; Wheeler, S. E. *J. Chem. Theory Comput.* **2012**, *8*, 3167−374.

(32) Morita, S. I.; Fujii, A.; Mikami, N.; Tsuzuki, S. *J. Phys. Chem. A* **2006**, *110*, 10583−10590.

(33) Fujii, A.; Shibasaki, K.; Kazama, T.; Itaya, R.; Mikami, N.; Tsuzuki, S. *Phys. Chem. Chem. Phys.* **2008**, *10*, 2836−2843.

(34) Saggu, M.; Levinson, N. M.; Boxer, S. G. *J. Am. Chem. Soc.* **2011**, *133*, 17414−17419.

(35) Saggu, M.; Levinson, N. M.; Boxer, S. G. *J. Am. Chem. Soc.* **2012**, *134*, 18986−18997.

(36) Bredas, J. L.; Street, G. B. *J. Chem. Phys.* **1989**, *90*, 7291−7299.

(37) Suzuki, S.; Green, P. G.; Bumgarner, R. E.; Dasgupta, S.; Goddard, W. A.; Blake, G. A. *Science* **1992**, *257*, 942−945.

(38) Gotch, A. J.; Zwier, T. S. *J. Chem. Phys.* **1992**, *96*, 3388−3401.

(39) Scheiner, S.; Kar, T.; Pattanayak, J. *J. Am. Chem. Soc.* **2002**, *124*, 13257−13264.

(40) Zheng, J.; Kwak, K.; Asbury, J.; Chen, X.; Piletic, I. R.; Fayer, M. D. *Science* **2005**, *309*, 1338−1343.

(41) Zheng, J.; Fayer, M. D. *J. Am. Chem. Soc.* **2007**, *129*, 4328−4335.

(42) Rosenfeld, D. E.; Gengeliczki, Z.; Fayer, M. D. *J. Phys. Chem. B* **2009**, *113*, 13300−13307.

(43) Read, W. G.; Campbell, E. J.; Henderson, G. *J. Chem. Phys.* **1983**, *78*, 3501−3508.

(44) Sanz, M. E.; Antolinez, S.; Alonso, J. L.; Lopez, J. C.; Kuczkowski, R. L.; Peebles, S. A.; Peebles, R. A.; Boman, F. C.; Kraka, E.; Cremer, D. *J. Chem. Phys.* **2003**, *118*, 9278−9290.

(45) Kim, K. S.; Lee, J. Y.; Choi, H. S.; Kim, J. S.; Jang, J. H. *Chem. Phys. Lett.* **1997**, *265*, 497−502.

(46) Tarakeshvar, P.; Lee, S. J.; Lee, J. Y.; Kim, K. S. *J. Chem. Phys.* **1998**, *108*, 7217−7223.

(47) Kim, K. S.; Tarakeshwar, P.; Lee, J. Y. *Chem. Rev.* **2000**, *100*, 4145−4185.

(48) Brutschy, B. *Chem. Rev.* **2000**, *100*, 3891−3920.

(49) (a) Mishra, B. K.; Karthikeyan, S.; Ramanathan, V. *J. Chem. Theory Comput.* **2012**, *8*, 1935−1942. (b) Karthikeyan, S.; Ramanathan, V.; Mishra, B. K. *J. Phys. Chem. A* **2013**, *113*, 6687−6694.

(50) Morokuma, K. *J. Chem. Phys.* **1971**, *55*, 1236−1244.

(51) Galabov, B.; Bobadova-Parvanova, P.; Ilieva, S.; Dimirrova, V. *J. Mol. Struct. (THEOCHEM)* **2003**, *630*, 101−112.

(52) Yoshida, Z.; Osawa, E. *J. Am. Chem. Soc.* **1966**, *88*, 4019−4026.

(53) Yoshida, Z.; Ishibe, N.; Kasumoto, H. *J. Am. Chem. Soc.* **1969**, *91*, 2279−2281.

(54) Yoshida, Z.; Ishibe, N.; Ozoe, H. *J. Am. Chem. Soc.* **1972**, *94*, 4948−4952.

(55) Seguin, J. P.; Nadjo, L.; Uzan, R.; Doucet, J. P. *Spectrochim. Acta, Part A* **1981**, *37A*, 205−210.

(56) Fujii, A.; Ebata, T.; Mikami, N. *J. Phys. Chem. A* **2002**, *106*, 8554−8560.

(57) (a) Becke, A. D. *J. Chem. Phys.* **1993**, *98*, 5648−5652. (b) Becke, A. D. *J. Chem. Phys.* **1996**, *104*, 1040−1046. (c) Lee, C. T.; Yang, W. T.; Parr, R. G. *Phys. Rev. B* **1988**, *37*, 785−789.

(58) Grimme, S. *J. Comput. Chem.* **2006**, *27*, 1787−1799.

(59) (a) Perdew, J. P.; Burke, K.; Ernzerhof, M. *Phys. Rev. Lett.* **1996**, *77*, 3865−3868. (b) Adamo, C.; Barone, V. *J. Chem. Phys.* **1999**, *110*, 6158−6169.

(60) (a) McLean, A. D.; Chandler, G. S. *J. Chem. Phys.* **1980**, *72*, 5639−5649. (b) Krishnan, R.; Binkley, J. S.; Seeger, R.; Pople, J. A. *J. Chem. Phys.* **1980**, *72*, 650−655. (c) Clark, T.; Chandrasekhar, J.; Spitznagel, G. W.; Schleyer, P. v. R. *J. Comput. Chem.* **1983**, *4*, 294−301.

(61) (a) Thanthiriwatte, K. S.; Hohenstein, E. G.; Burns, L. A.; Sherrill, C. D. *J. Chem. Theor. Comp.* **2011**, *7*, 88−96. (b) Neves, A. R.; Fernandes, P. A.; Ramos, M. J. *J. Chem. Theory Comput.* **2011**, *7*, 2059−2067. (c) Zhao, Y.; Tishchenko, O.; Truhlar, D. G. *J. Phys. Chem. B* **2005**, *109*, 19046−19051. (d) Wijst, T. V. D.; Guerra, C. F.; Swart, M.; Bickelhaupt, F. M. *Chem. Phys. Lett.* **2006**, *426*, 415−421.

(62) Boys, S. F.; Bernardi, F. *Mol. Phys.* **1970**, *19*, 553−566.

(63) Tomasi, J.; Mennucci, B.; Cammi, R. *Chem. Rev.* **2005**, *105*, 2999−3093.

(64) Frisch, M. J. et al. *Gaussian09 (Revision-A.02)*; Gaussian, Inc., Wallingford, CT, 2009.

(65) (a) Reed, A. E.; Weinstock, R. B.; Weinhold, F. *J. Chem. Phys.* **1985**, *83*, 735−746. (b) Reed, A. E.; Curtiss, L. A.; Weinhold, F. *Chem. Rev.* **1988**, *88*, 899−926.

(66) (a) Hirshfeld, F. L. *Theor. Chem. Acc.* **1977**, *44*, 129−138. (b) Ritchie, J. P. *J. Am. Chem. Soc.* **1985**, *107*, 1829−1835. (c) Ritchie, J. P.; Bachrach, S. M. *J. Comput. Chem.* **1987**, *8*, 499−509.

(67) *Chemical Applications of Atomic and Molecular Electrostatic Potentials*, Politzer, P., Truhlar, D. G., Eds.; Plenum Press: New York, 1981.

(68) (a) Bobadova-Parvanova, P.; Galabov, B. *J. Phys. Chem. A* **1998**, *102*, 1815−1819. (b) Galabov, B.; Bobadova-Parvanova, P. *J. Phys. Chem. A* **1999**, *103*, 6793−6799.

(69) (a) Galabov, B.; Bobadova-Parvanova, P. *J. Mol. Struct. (THEOCHEM)* **2000**, *550−551*, 93−98. (b) Dimitrova, V.; Ilieva, S.; Galabov, B. *J. Phys. Chem. A* **2002**, *106*, 11801−11805. (c) Galabov, B.; Bobadova-Parvanova, P.; Ilieva, S.; Dimitrova, V. *J. Mol. Struct. (THEOCHEM)* **2003**, *630*, 101−112.

(70) (a) Galabov, B.; Cheshmedzhieva, D.; Ilieva, S.; Hadjieva, B. *J. Phys. Chem. A* **2004**, *108*, 11457−11462. (b) Galabov, B.; Ilieva, S.; Schaefer, H. F. *J. Org. Chem. A* **2006**, *71*, 6382−6387. (c) Galabov, B.; Ilieva, S.; Hadjieva, B.; Atanasov, Y.; Schaefer, H. F. *J. Phys. Chem. A* **2008**, *112*, 6700−6707. (d) Galabov, B.; Nikolova, V.; Wilke, J. J.; Schaefer, H. F.; Allen, W. D. *J. Am. Chem. Soc.* **2008**, *130*, 9887−9896. (e) Galabov, B.; Ilieva, S.; Koleva, G.; Allen, W. D.; Schaefer, H. F.; Schleyer, P. v. R. *WIREs Comp. Mol. Sci.* **2013**, *3*, 37−55. (f) Ilieva, S.; Nalbantova, D.; Hadjieva, B.; Galabov, B. *J. Org. Chem.* **2013**, *78*, 6440−6449.

(71) (a) Sayyed, F. B.; Suresh, C. H. *Tetrahedron Lett.* **2009**, *50*, 7351−7354. (b) Zeng, Y.; Xue, Y.; Yan, G. *J. Phys. Chem. A* **2011**, *115*, 4995−5004. (c) Sadlej-Sosnowska, N. *Chem. Phys. Lett.* **2007**, *447*, 192−196. (d) Alia, J. M.; Edwards, H. G. *J. Phys. Chem. A* **2005**, *109*, 7977−7987. (e) Alia, J. M.; Edwards, H. G. *Int. J. Quantum Chem.* **2007**, *107*, 1170−1180. (f) Karpfen, A.; Kryachko, E. S. *J. Phys. Chem. A* **2005**, *109*, 8930−8937. (g) Zheng, W. X.; Wong, N. B.; Li, W. K. *J. Phys. Chem. A* **2004**, *108*, 11721−11727. (h) Sadlej-Sosnowska, N.; Murlowska, K. *J. Phys. Chem. A* **2008**, *112*, 10017−10022. (i) Novakovic, S. B.; Fraisse, B.; Bogdanovic, G. A.; Ghermani, N. E.; Bouhmaida, N.; Spasojevic-de Bire, A. *J. Phys. Chem. A* **2007**, *111*, 13492−13505. (j) Bhattacharjee, R.; Roy, K. *J. Phys. Chem. A* **2013**, *117*, 11528−11539. (k) Papp, T.; Kollar, L.; Kegl, T. *Chem. Phys. Lett.* **2013**, *588*, 51−56. (l) Graton, J.; Besseau, F.; Brossard, A.-M.; Charpentier, E.; Deroche, A.; Le Questel, J.-Y. *J. Phys. Chem. A* **2013**, *117*, 13184−13193.

(72) Galabov, B.; Nikolova, V.; Ilieva, S. *Chem. Eur. J.* **2013**, *19*, 5149−5155.

(73) (a) Szatylowicz, H.; Krygowski, T. M. *J. Phys. Org. Chem.* **2009**, *22*, 740−746. (b) Szatylowicz, H.; Krygowski, T. M. *J. Phys. Chem. A* **2010**, *114*, 10885−10890.

(74) Hobza, P.; Havlas, Z. *Chem. Rev.* **2000**, *100*, 4253−4264.

(75) (a) Hammett, L. P. *Physical Organic Chemistry*, 2nd ed.; McGraw-Hill: New York, 1970. (b) Hansch, C.; Leo, A.; Taft, R. W. *Chem. Rev.* **1991**, *91*, 1062−1080.

(76) (a) Dean, J. A. *Lange's Handbook of Chemistry*, 15th ed.; McGraw-Hill: New York, 1999. (b) Bartmess, J. E. Negative Ion Energetics Data. In *NIST Chemistry WebBook*; Mallard, W. G., Lindstrom, P. J., Eds.; National Institute of Standards and Technology: Gaithersburg, MD, 2005; NIST Standard Reference Database Number 69, http://webbook.nist.gov.